Inorg. Chem. **2004**, *43*, 725–733

Tuning the Electronic Structures of Platinum(II) Complexes with a Cyclometalating Aryldiamine Ligand

Hershel Jude, Jeanette A. Krause Bauer, and William B. Connick*

Department of Chemistry, University of Cincinnati, P.O. Box 210172, Cincinnati, Ohio 45221-0172

Received June 6, 2003

Triflate salts of four platinum(II) pyridyl complexes with a *mer*-coordinating tridentate pincer ligand, pip_2NCN^- (pip_2-NCNH = 1,3-bis(piperidylmethyl)benzene), are reported: $Pt(pip_2NCN)(L)^+$ (**2**, L = pyridine; **3**, L = 4-phenylpyridine; **5**, L = 2,6-pyridinedimethanol) and $[(Pt(pip_2NCN))_2(\mu\text{-}4,4'\text{-bipyridine})]^{2+}$ (**4**). The complexes have been fully characterized by ^{1}H NMR spectroscopy, elemental analysis, and X-ray crystallography. Compound **2**($CF_3SO_3^-$): triclinic, $P\bar{1}$, a = 9.7518(6) Å, b = 12.0132(8) Å, c = 12.6718(9) Å, α = 114.190(2)°, β = 100.745(3)°, γ = 103.545(2)°, V = 1247.95(14) Å^3, Z = 2. Compound **3**($CF_3SO_3^-$): monoclinic, $P2_1/c$, a = 15.550(2) Å, b = 9.7386(11) Å, c = 18.965(3) Å, β = 92.559(7)°, V = 2869.1(6) Å^3, Z = 4. Compound **4**($CF_3SO_3^-)_2\cdot 1/2(CH_3)_2CO$: monoclinic, $I2/a$, a = 21.3316(5) Å, b = 9.6526(2) Å, c = 26.1800(6) Å, β = 96.4930(10)°, V = 5356.0(2) Å^3, Z = 4. Compound **5**($CF_3SO_3^-)\cdot 3/2CHCl_3$: monoclinic, $P2_1/n$, a = 17.1236(10) Å, b = 9.3591(5) Å, c = 21.3189(11) Å, β = 96.11(3)°, V = 3397.2(3) Å^3, Z = 4. The accumulated data indicate that the phenyl group of pip_2NCN^- labilizes the trans pyridyl ligand. The electronic structures were investigated using cyclic voltammetry, as well as UV–visible absorption and emission spectroscopies. Red emission from **2** in rigid media originates from a lowest triplet ligand field excited state, whereas yellow-green emissions from **3** and **4** originate from a lowest pyridyl ligand-centered triplet π–π^* state, indicating that substitution of the pyridyl ligand results in a dramatic change in the orbital character of the emissive state.

Introduction

Platinum complexes with tridentate cyclometalating aryldiamine ligands, such as the 2,6-bis((dimethylamino)methyl)-phenyl anion (Me_4NCN^-), have attracted increasing interest, in part because of their potential utility in gas-sensing devices,[1] catalytic systems,[2] and the preparation of organometallic supramolecular structures and materials.[3,4]

In an effort to better understand the electronic structures of platinum(II) complexes with NCN^- ligands, we recently undertook an investigation of the emissive properties of a series of complexes with the pip_2NCN^- pincer ligand.[5] It was found that compounds with the general formula $Pt(pip_2NCN)X$ (X = Cl, Br, I), as well as $Pt(pip_2NCN)(CH_3N{=}C(CH_3)_2)^+$, exhibit weak, red emissions originating from a lowest predominantly spin-forbidden ligand field (^{3}LF) excited state. More recently, a series of related complexes were prepared with monodentate pyridyl ligands. In the course of these studies, it was noted that $Pt(pip_2NCN)(py)^+$ (py = pyridine) exhibits red emission characteristic of a lowest ^{3}LF excited state. In contrast, $Pt(pip_2NCN)(4\text{-phpy})^+$ (4-phpy = 4-phenylpyridine) exhibits intense yellow-green emission. Here, we report the synthesis and characterization

* To whom correspondence should be addressed. E-mail: bill.connick@uc.edu.

(1) (a) Albrecht, M.; Gossage, R. A.; van Koten, G.; Spek, A. L. *Chem. Commun.* **1998**, 1003−1004. (b) Albrecht, M.; Lutz, M.; Spek, A. L.; van Koten, G. *Nature* **2000**, *406*, 970−974. (c) Albrecht, M.; Hovestad, N. J.; Boersma, J.; van Koten, G. *Chem.−Eur. J.* **2001**, *7*, 1289−1294.

(2) (a) Gorla, F.; Togni, A.; Venanzi, L. M.; Albinati, A.; Lianza, F. *Organometallics* **1994**, *13*, 1607−1616. (b) Motoyama, Y.; Mikami, Y.; Kawakami, H.; Aoki, K.; Nishiyama, H. *Organometallics* **1999**, *18*, 3584−3588. (c) Motoyama, Y.; Kawakami, H.; Shimozono, K.; Aoki, K.; Nishiyama, H. *Organometallics* **2002**, *21*, 3408−3416.

(3) (a) Davies, P. J.; Veldman, N.; Grove, D. M.; Spek, A. L.; Lutz, B. T. G.; van Koten, G. *Angew. Chem., Int. Ed. Engl.* **1996**, *35*, 1959−1961. (b) James, S. L.; Verspui, G.; Spek, A. L.; van Koten, G. *Chem. Commun.* **1996**, *11*, 1309−1310. (c) Steenwinkel, P.; Kooijman, H.; Smeets, W. J. J.; Spek, A. L.; Grove, D. M.; van Koten, G. *Organometallics* **1998**, *17*, 5411−5426. (d) Rodriguez, G.; Albrecht, M.; Schoenmaker, J.; Ford, A.; Lutz, M.; Spek, A. L.; van Koten, G. *J. Am. Chem. Soc.* **2002**, *124*, 5127−5138.

(4) For a recent review, see Albrecht, M.; van Koten, G. *Angew. Chem., Int. Ed.* **2001**, *40*, 3750−3781.

(5) Jude, H.; Krause Bauer, J. A.; Connick, W. B. *Inorg. Chem.* **2002**, *41*, 2275−2281.

10.1021/ic0346329 CCC: $27.50
Published on Web 12/18/2003

of a series of complexes with pyridyl ligands and examine the influence of the pyridyl ligand on the orbital character of the lowest emissive state.

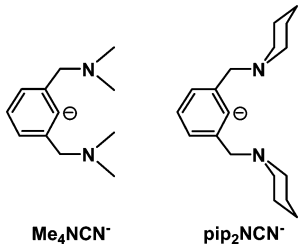

Experimental Section

All reagents were purchased from Acros. Tetrahydrofuran (THF) was distilled from Na(s) and benzophenone, ethanol was distilled from zinc metal and potassium hydroxide, and methylene chloride was distilled over CaH_2. All other chemicals were used as received. $Pt(COD)Cl_2$[6] and 2,6-bis(piperdylmethyl)-1-bromobenzene (pip_2NCNBr)[5] were prepared according to literature procedures. Tetrabutylammonium hexafluorophosphate ($(TBA)PF_6$) was recrystallized twice from boiling methanol and dried under vacuum prior to use. Argon was predried using activated sieves, and trace impurities of oxygen were removed with activated R3-11 catalyst from Schweizerhall.

^1H NMR spectra were recorded at room temperature, unless otherwise noted, using a Bruker AC 250 MHz spectrometer. Deuterated chloroform (0.03% tetramethylsilane (TMS)), methanol, and acetonitrile were purchased from Cambridge Isotope Laboratories. UV−vis spectra were recorded using a HP8453 UV−visible spectrometer. Cyclic voltammetery was carried out using a standard three-electrode cell and a CV50w potentiostat from Bioanalytical Systems. Scans were collected in methylene chloride solution containing 0.1 M $(TBA)PF_6$. All scans were recorded using a platinum wire auxiliary electrode, a Ag/AgCl (3.0 M NaCl), reference electrode, and a 0.79 mm^2 gold working electrode. Between scans, the working electrode was polished with 0.05 μm alumina, rinsed with distilled water, and wiped dry using a Kimwipe. The values of $(E_{pc} + E_{pa})/2$, which is an approximation of the formal potential for a redox couple, are referred to as $E^{\circ\prime}$. Reported potentials are referenced against Ag/AgCl. Peak currents (i_p) were estimated with respect to the extrapolated baseline current as described elsewhere.[7] Under these conditions, the ferrocene/ferrocenium (FcH/FcH^+) couple occurs at 0.45 V.

Emission spectra were recorded as previously described.[5] Emission samples for lifetime measurements at 77 K were excited using the third harmonic (355 nm) of a Continuum Surelite Nd:YAG with 4−6 ns pulse widths. Emission transients were detected using a modified PMT connected to a Tektronix TDS580D oscilloscope and modeled using in-house software on a Microsoft Excel platform. Under these conditions, the emission decay of $[Ru(bpy)_3]Cl_2$ in a 4:1 EtOH−MeOH 77 K glassy solution was single exponential corresponding to a 5.1 μs lifetime, as expected.[8]

Pt(pip$_2$NCN)Cl (1). All glassware and compounds were rigorously dried prior to use because this reaction was found to be extremely sensitive to moisture. Under an Ar(g) atmosphere, 1.84 mL (3.0 mmol) of *N*-butyllithium (1.6 M in hexanes) was added to a stirred solution of pip_2NCNBr (1.13 g, 3.2 mmol) in 50 mL of THF at −70 °C. After 30 min, the solution of lithiated ligand was cannula transferred into a mixture of $Pt(COD)Cl_2$ (1.0 g, 2.7 mmol) in 200 mL THF at −70 °C. The mixture was stirred for 1 h at −70 °C and subsequently allowed to warm to room temperature and stirred for 12 h. The filtrate was rotoevaporated to dryness. Water was added to the solid, and the product was extracted with CH_2Cl_2. The organic layer was dried over $MgSO_4$ and rotoevaporated to dryness. After addition of hexanes to the precipitate, the mixture was sonicated, and the white solid was collected and dried. Yield: 1.1 g, 82%. Anal. Calcd for $C_{18}H_{27}N_2PtCl$: C, 43.08; H, 5.42; N, 5.58. Found: C, 42.98; H, 5.44; N, 5.43. ^1H NMR ($CDCl_3$, δ): 1.43 (4H, m, CH_2), 1.54−1.79 (8H, m, CH_2), 3.25 (4H, m, CH_2), 3.95 (4H, m, CH_2), 4.25 (4H, s with Pt satellites, $J_{H-Pt} = 47$ Hz, benzylic CH_2), 6.80 (2H, d, CH), and 6.98 (1H, t, CH).

[Pt(pip$_2$NCN)(py)][CF$_3$SO$_3$] (2(CF$_3$SO$_3^-$)). A mixture of silver triflate (0.052 g, 0.20 mmol) and **1** (0.10 g, 0.20 mmol) in 15 mL of acetone was stirred for 30 min at room temperature. The resulting AgCl precipitate was removed by vacuum filtration through Celite. After addition of pyridine (15 μL, 0.20 mmol), the filtrate was stirred for 3 h, and the solvent was removed by rotary evaporation. The white solid was dissolved in CH_2Cl_2, and hexanes were added to induce precipitation. The product was washed with ether and dried. Yield: 0.095 g, 82%. Anal. Calcd for $[C_{23}H_{32}N_3Pt]][CF_3SO_3]$: C, 41.50; H, 4.64; N, 6.05. Found: C, 41.65; H, 4.77; N, 6.12. ^1H NMR ($CDCl_3$, δ): 1.17−1.24 (4H, m, CH_2), 1.60−1.83 (8H, m, CH_2), 2.90 (4H, m, CH_2), 3.27 (4H, m, CH_2), 4.39 (4H, s with Pt satellites, $J_{H-Pt} = 54$ Hz, benzylic CH_2), 6.91 (2H, d, CH), 7.05 (1H, t, CH), 7.85 (2H, dd, CH), 8.04 (1H, t, CH), and 9.01 (2H, d, CH).

[Pt(pip$_2$NCN)(4-phpy)][CF$_3$SO$_3$] (3(CF$_3$SO$_3^-$)). This was prepared by the same procedure as **2**, substituting the appropriate starting materials: **1** (0.050 g, 0.10 mmol); silver triflate (0.026 g, 0.10 mmol); 4-phenylpyridine (0.016 g, 0.10 mmol). Yield: 0.045 g, 58%. Anal. Calcd for $[C_{29}H_{36}N_3Pt]][CF_3SO_3]\cdot H_2O$: C, 45.68; H, 4.85; N, 5.33. Found: C, 45.66; H, 4.67; N, 5.34. ^1H NMR ($CDCl_3$, δ): 1.26−1.31 (4H, m, CH_2), 1.62−1.78 (8H, m, CH_2), 2.98 (4H, m, CH_2), 3.32 (4H, m, CH_2), 4.40 (4H, s with Pt satellites, $J_{H-Pt} = 50$ Hz, benzylic CH_2), 6.92 (2H, d, CH), 7.54 (3H, m, CH), 7.85 (2H, m, CH), 8.05 (2H, d, CH), and 9.05 (2H, d, CH).

[Pt(pip$_2$NCN)(4-phpy)][BF$_4$] (3(BF$_4^-$)). This was prepared by the same procedure as for the triflate salt, substituting $AgBF_4$ for silver triflate. Yield: 74%. Anal. Calcd for $[C_{29}H_{36}N_3Pt]][BF_4]\cdot H_2O$: C, 47.94; H, 5.27; N, 5.78. Found: C, 47.99; H, 4.94; N, 5.54.

[(Pt(pip$_2$NCN))$_2$(μ-4,4′-bpy)][CF$_3$SO$_3$]$_2$ (4(CF$_3$SO$_3^-$)$_2$). This was prepared by the same procedure as for **2**, substituting the appropriate starting materials: **1** (0.10 g, 0.20 mmol); silver triflate (0.052 g, 0.20 mmol); 4,4′-bipyridine (4,4′-bpy, 0.0155 g, 0.10 mmol). Yield: 0.078 g, 57%. Anal. Calcd for $[C_{46}H_{62}N_6Pt_2]][CF_3SO_3]_2$: C, 41.55; H, 4.50; N, 6.06. Found: C, 41.89; H, 4.51; N, 6.31. ^1H NMR ($CDCl_3$, δ): 1.25−1.35 (8H, m, CH_2), 1.58−1.1.80 (16H, m, CH_2), 2.95 (8H, m, CH_2), 3.30 (8H, m, CH_2), 4.41 (8H, s with Pt satellites, $J_{H-Pt} = 47$ Hz, benzylic CH_2), 6.93 (4H, d, CH), 7.07 (2H, t, CH), 8.63 (4H, d, CH), and 9.10 (4H, d, CH).

[Pt(pip$_2$NCN)(2,6-pydiol)][CF$_3$SO$_3$] (5(CF$_3$SO$_3^-$)). This was prepared by the same procedure as for **2**, except stirring for 12 h and substituting the appropriate starting materials: **1** (0.078 g, 0.15 mmol); silver triflate (0.040 g, 0.15 mmol); 2,6-pyridinedimethanol (2,6-pydiol, 0.022 g, 0.15 mmol). Yield: 0.100 g, 89%. Anal. Calcd for $[C_{25}H_{36}N_3O_2Pt]][CF_3SO_3]$: C, 41.37; H, 4.81; N, 5.57. Found: C, 41.12; H, 4.61; N, 5.46. ^1H NMR ($CDCl_3$, δ, 242 K): 1.75 (4H,

(6) McDermott, J. X.; White, J. F.; Whitesides, G. M. *J. Am. Chem. Soc.* **1976**, *98*, 6521−6528.
(7) Kissinger, P. T.; Heineman, W. R. *J. Chem. Educ.* **1983**, *60*, 702−706.
(8) Juris, A.; Belser, P.; Barigelletti, F.; von Zelewsky, A.; Balzani, V. *Inorg. Chem.* **1988**, *25*, 256−259.

Scheme 1[a]

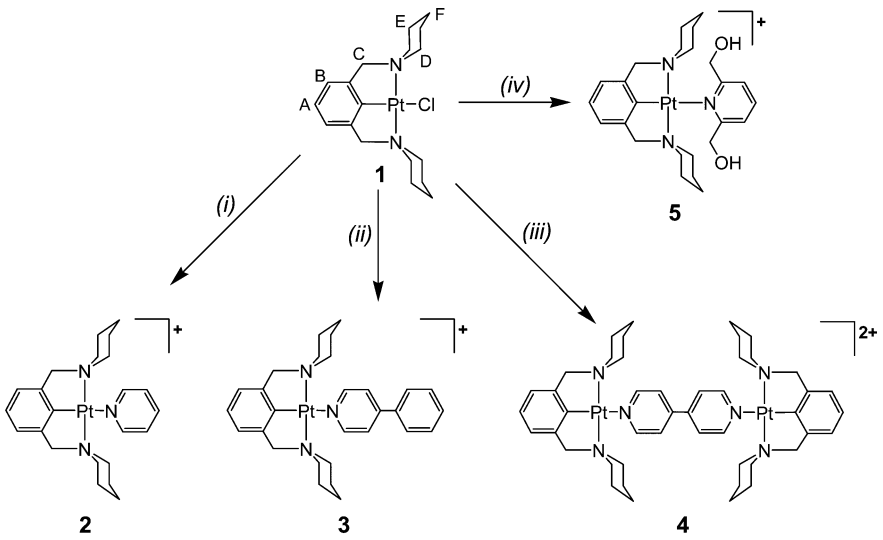

[a] Key: (i) $AgCF_3SO_3$, pyridine, acetone; (ii) $AgCF_3SO_3$, 4-phenylpyridine, acetone; (iii)$AgCF_3SO_3$, 4,4′-bipyridine, acetone; (iv) $AgCF_3SO_3$, 2,6-pydiol, acetone.

m, CH_2), 1.27 (8H, m, CH_2), 2.76 (4H, m, CH_2), 3.35 (4H, m, CH_2), 4.42 (4H, s, benzylic CH_2), 5.33 (2H, t, OH), 5.80 (4H, d, benzylic CH_2), 6.96 (2H, d, CH), 7.11 (1H, t, CH), 7.94 (2H, d, CH), and 8.05 (1H, t, CH).

X-ray Crystallography. Yellow rods of **2**($CF_3SO_3^-$) were grown by slow evaporation of an acetone solution. Colorless rectangular plates of **3**($CF_3SO_3^-$) were grown by slow evaporation of a CH_2Cl_2−hexanes solution. Colorless plates of **4**$(CF_3SO_3^-)_2 \cdot 1/2(CH_3)_2CO$ were grown by slow evaporation of an acetone−hexanes solution. Colorless rods of **5**($CF_3SO_3^-$)·3/2$CHCl_3$ were grown by slow evaporation of a chloroform solution. Diffraction data were collected at 150 K on a Siemens SMART 1K CCD diffractometer (Mo Kα radiation and graphite monochromator, $\lambda = 0.710\ 73$ Å). Data frames were processed using the Bruker SAINT program.[9] Intensities were corrected for Lorentz, polarization, and decay effects. Absorption and beam corrections based on the multiscan technique were applied using SADABS.[10] The structures were solved using SHELXTL v5.03[11] and refined by full-matrix least squares on F^2. For all compounds non-hydrogen atoms were located directly by successive Fourier calculations and refined anisotropically. Ligand H atoms were calculated on the basis of geometric criteria and were treated with a riding model in subsequent refinements for **2**−**4**. For **5**($CF_3SO_3^-$)·3/2$CHCl_3$, the hydroxyl H atoms were located directly and held fixed at that location. The remaining H atoms were either located directly or calculated on the basis of geometric criteria and were treated with a riding model in subsequent refinements. The isotropic displacement parameters for the H atoms were defined as a times U_{eq} of the adjacent atom, where $a = 1.5$ for $-CH_3$ and 1.2 for all others. For **2**($CF_3SO_3^-$), the anion is disordered, and a suitable model could not be constructed. Its contribution was subtracted from the data using the program SQUEEZE.[12] The final difference Fourier map showed a highest residual electron density peak (1.79 e $Å^{-3}$) within 1 Å of the Pt. Compound **4**$(CF_3SO_3^-)_2$ crystallizes with a badly disordered solvent molecule, which appears to be acetone (∼50% occupancy). A suitable disorder model was not obtained, and the solvent contribution was subtracted from the reflection data using the program SQUEEZE.[12] The 58.2 electrons/unit cell were applied to the molecular weight, $F(000)$, and density values reported. Compound **5**($CF_3SO_3^-$) crystallizes with 3/2 $CHCl_3$ in the lattice. The fully occupied $CHCl_3$ refines normally, but the partially occupied molecule of $CHCl_3$ is disordered about a center of symmetry. The refined occupancy for the chlorine atoms was approximately 50% and rounded to 0.5 in subsequent refinements. The carbon atom adopts two positions with occupancies of 0.3 and 0.2.

Results and Discussion

Synthesis. The synthesis of **1**−**5** is illustrated in Scheme 1, and the pyridyl complexes were isolated as triflate salts. The colorless compounds were characterized by ^1H NMR spectroscopy and elemental analysis. Previously we reported the preparation of **1** from $Pt(SMe_2)_2Cl_2$, using chromatography to obtain product in low yields (∼40%).[5] Here we report a slightly modified procedure for the conversion of $Pt(COD)Cl_2$ to product in much higher yields (75−82%) without chromatography. Isolation of salts of **2**−**5** also is straightforward, giving good yields. Methathesis was accomplished by allowing compound **1** to react with a silver salt (e.g., $AgCF_3SO_3$) at room temperature. After removal of silver chloride by filtration, 1 equiv of pyridine, 4-phenylpyridine, or 2,6-pyridinedimethanol was added to give **2**, **3**, or **5**, respectively. In the case of **4**, 0.5 equiv of 4,4′-bipyridine were used.

Crystal Structures. The structures of the triflate salts of **2**−**5** were confirmed by single-crystal X-ray diffraction studies. ORTEP diagrams of the cations are shown in Figure 1, and relevant data are summarized in Tables 1 and 2. No

(9) Bruker SMART v5.051 and v5.622 and SAINT v5.A06 programs were used for data collection and data processing, respectively: Bruker Analytical X-ray Instruments, Inc., Madison, WI.

(10) SADABS was used for the application of semiempirical absorption and beam corrections for the CCD data: G. M. Sheldrick, University of Goettingen, Goettingen, Germany, 1996.

(11) SHELTX v5.03 was used for the structure solution and generation of figures and tables: G. M. Sheldrick, University of Goettingen, Germany, and Siemens Analytical X-ray Instruments, Inc., Madison, WI.

(12) Spek, A. L. University of Utrecht, Utrecht, The Netherlands, 1992. SQUEEZE is a routine implemented in PLATON-92 allowing solvent contributions to be eliminated from the reflection data.

unusual intermolecular interactions are present, and there is no evidence of water molecules in any of the crystals. For each complex, the pip_2NCN^- ligand is tridentate, bonded to the approximately square planar platinum center. Each piperidyl ring adopts a chair conformation with the Pt atom occupying an equatorial site. As a result, the piperidyl rings are splayed away from the pyridyl ligands and do not appear to interfere with coordination to platinum. The pyridyl groups adopt an approximately perpendicular orientation to the platinum coordination plane.

The Pt−C and Pt−N(piperidyl) distances for **2** (1.920(4) Å; 2.104(3), 2.092(3) Å), **3** (1.917(3) Å; 2.103(3), 2.099(3) Å), **4** (1.926(5) Å; 2.107(5), 2.098(5) Å), and **5** (1.930(2) Å; 2.124(2), 2.117(2) Å) are consistent with those of related complexes with the same tridentate ligand, $Pt(pip_2NCN)Cl$ (1.910(4), 1.899(5) Å; 2.094(3), 2.099(3), 2.101(4), 2.115(4) Å) and $Pt(pip_2NCN)(CH_3N{=}C(CH_3)_2)][CF_3SO_3]$ (1.919(5) Å; 2.108(3), 2.104(3) Å).[5] The Pt−N(pyridyl) distances (**2**, 2.159(3) Å; **3**, 2.143(3) Å; **4**, 2.138 (4) Å) are significantly longer than the distances for pyridyl ligands trans to a weaker trans-directing ligand such as ethylenediamine ($[(Pt(ethylene\text{-}1,2\text{-}diamine)(4,4'\text{-}bpy))_4]^{8+}$, 2.012, 2.013, 2.041, 2.044 Å)[13] but agree with those observed when the pyridyl ligand is trans to a relatively strong trans-directing group such as phenyl anion ($[(Pt(PEt_3)_2)_4(4,4'\text{-}bpy)_2(anthracenyl)_2]^{4+}$, 2.132(5), 2.138(6) Å;[14] $Pt((2,6\text{-}CH_2PPh_2)_2C_6H_3)(8\text{-}acetamidoquinolinato)^+$, 2.150(4) Å).[15] For **5**, the Pt−N(pyridyl) distance (2.201(2) Å) is significantly longer than those found for **2**−**4** and the N(pyridyl)−Pt−N(piperidyl) angles are smaller, suggesting the steric demands of the piperidyl and pyridinedimethanol groups interfere with coordination to the metal center.

The N(piperidyl)−Pt−N(piperidyl) angles (**2**, 164.45(12)°; **3**, 164.12(11)°; **4**, 162.4(2)°; **5**, 161.20(8)°) substantially deviate from ideal trans-coordination, with **5** exhibiting the smallest value. This deviation has been ascribed to the geometric preferences of the two five-membered chelate rings.[16,17] For **2**−**5**, the rings are slightly puckered, resulting in displacement of the benzylic carbons above and below (**2**, 0.113, 0.321 Å; **3**, 0.603, 0.537 Å; **4**, 0.744, 0.677 Å; **5**, 0.701, 0.693 Å) the platinum coordination plane, defined by the four atoms directly bonded to platinum center. The displacements for **2** lie outside the range of observed values for related compounds (0.492−0.702 Å).[5] To accommodate this puckering, the planar phenyl ring is rotated slightly about the Pt−C bond, forming dihedral angles (**2**, 7.6°; **3**, 11.6°; **4**, 15.6°; **5**, 14.41°) with the Pt coordination plane. These twist angles are similar to those found for other complexes with the pip_2NCN^- ligand, $Pt(pip_2NCN)Cl$ (10.3, 9.2°) and $Pt(pip_2NCN)(CH_3N{=}C(CH_3)_2$ (11.4°).[5] The variability in

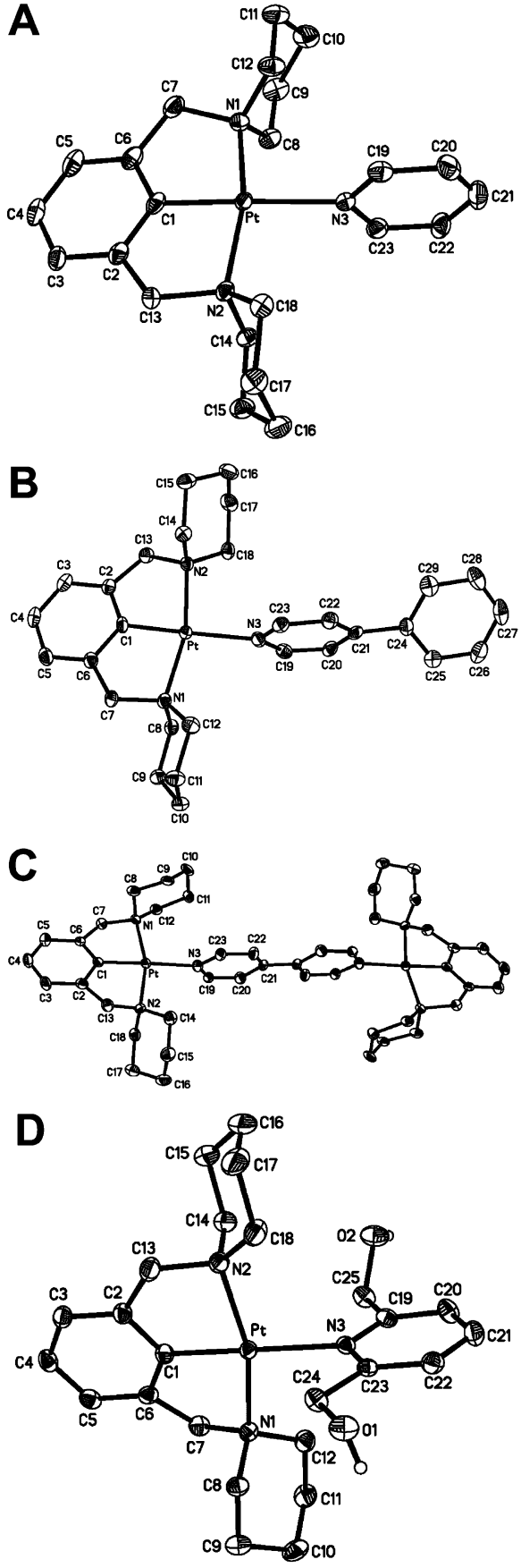

Figure 1. ORTEP diagrams of the cations in crystals of (A) **2**($CF_3SO_3^-$), (B) **3**($CF_3SO_3^-$), (C) **4**($CF_3SO_3^-$)$_2$·1/2(CH_3)$_2$CO, and (D) **5**($CF_3SO_3^-$)·3/2$CHCl_3$. H atoms are omitted for clarity, with the exception of hydroxyl groups of **5**.

(13) Aoyagi, M.; Biradha, K.; Fujita, M. *Bull. Chem. Soc. Jpn.* **1999**, *72*, 2603−2606.
(14) Kuehl, C. J.; Arif, A. M.; Stang, P. J. *Org. Lett.* **2000**, *2*, 3727−3729.
(15) Albinati, A.; Lianza, F.; Pregosin, P. S.; Muller, B. *Inorg. Chem.* **1994**, *33*, 2522−2526.
(16) Schmulling, M.; Grove, D. M.; van Koten, G.; van Eldik, R.; Veldman, N.; Spek, A. L. *Organometallics* **1996**, *15*, 1384−1391.
(17) Donkervoort, J. G.; Vicario, J. L.; Jastrzebski, J. T. B. H.; Smeets, W. J. J.; Spek, A. L.; van Koten, G. *J. Organomet. Chem.* **1998**, *551*, 1−7.

Table 1. Crystallographic Data and Structural Refinement Details for Compounds **2**($CF_3SO_3^-$), **3**($CF_3SO_3^-$), **4**($CF_3SO_3^-$)$_2$·1/2$(CH_3)_2CO$, and **5**($CF_3SO_3^-$)·3/2$CHCl_3$

	2($CF_3SO_3^-$)	**3**($CF_3SO_3^-$)	**4**($CF_3SO_3^-$)$_2$·1/2$(CH_3)_2CO$	**5**($CF_3SO_3^-$)·3/2$CHCl_3$
formula	$[C_{23}H_{32}N_3Pt][CF_3SO_3]$	$[C_{29}H_{36}N_3Pt][CF_3SO_3]$	$[C_{46}H_{62}N_6Pt_2][CF_3SO_3]_2$·1/2$(CH_3)_2CO$	$[C_{25}H_{36}N_3O_2\ Pt][CF_3SO_3]$·3/2$CHCl_3$
fw	694.68	770.77	1387.34	933.78
space group	$P\bar{1}$	$P2_1/c$	$I2/a$	$P2_1/n$
a, Å	9.7518(6)	15.550(2)	21.3316(5)	17.1236(10)
b, Å	12.0132(8)	9.7386(11)	9.6526(2)	9.3591(5)
c, Å	12.6718(9)	18.965(3)	26.1800(6)	21.3189(11)
α, deg	114.190(2)	90	90	90
β, deg	100.745(3)	92.559(7)	96.4930(10)	96.11(3)
γ, deg	103.545(2)	90	90	90
V, Å^3	1247.895(14)	2869.1(6)	5356.0(2)	3397.2(3)
Z	2	4	4	4
ρ_{calc}, g cm^{-3}	1.849	1.784	1.720	1.826
T, K	150(2)	150(2)	150(2)	150(2)
radiation, Å	0.710 73	0.710 73	0.710 73	0.710 73
no. of reflcns collcd	13 294	18 166	26 659	34 572
no. of indpt reflcns	6024	7016	6614	8379
GOF on F^2	1.090	0.961	1.143	1.006
R_1/wR_2 [$I > 2\sigma(I)$][a]	0.0262/0.0704	0.0273/0.0528	0.0451/0.0776	0.0210/0.0468
R_1/wR_2 (all data)[a]	0.0289/0.0711	0.0430/0.0566	0.0758/0.0860	0.0293/0.0486

[a] $R_1 = \sum||F_o| - |F_c||/\sum|F_o|$, $wR_2 = [\sum w(F_o^2 - F_c^2)^2/\sum w(F_o^2)^2]^{1/2}$.

Table 2. Selected Distances (Å) and Angles (deg) for Compounds **2**($CF_3SO_3^-$), **3**($CF_3SO_3^-$), **4**($CF_3SO_3^-$)$_2$·1/2$(CH_3)_2CO$, and **5**($CF_3SO_3^-$)·3/2$CHCl_3$

	2($CF_3SO_3^-$)	**3**($CF_3SO_3^-$)	**4**($CF_3SO_3^-$)$_2$·1/2$(CH_3)_2CO$	**5**($CF_3SO_3^-$)·3/2$CHCl_3$
Pt−C(1)	1.920(4)	1.917(3)	1.926(5)	1.930(2)
Pt−N(1)	2.104(3)	2.103(3)	2.107(5)	2.124(2)
Pt−N(2)	2.092(3)	2.099(3)	2.098(5)	2.117(2)
Pt−N(3)	2.159(3)	2.143(3)	2.138(4)	2.201(2)
N(1)−C(7)	1.531(5)	1.528(4)	1.534(7)	1.529(3)
N(2)−C(13)	1.536(5)	1.528(4)	1.534(7)	1.523(3)
C(6)−C(7)	1.493(6)	1.499(6)	1.500(8)	1.507(3)
C(2)−C(13)	1.503(5)	1.510(5)	1.513(8)	1.502(3)
C(1)−Pt−N(2)	82.7(2)	81.68 (13)	81.5(2)	80.45(9)
C(1)−Pt−N(1)	83.1(2)	82.54 (13)	80.8(2)	81.23(9)
C(1)−Pt−N(3)	176.67(13)	177.34(12)	178.4(2)	177.15(8)
N(2)−Pt−N(1)	164.45(12)	164.12(11)	162.4(2)	161.20(8)
C(7)−N(1)−Pt	109.5(2)	106.0(2)	105.2(3)	105.36(13)
C(13)−N(2)−Pt	108.5(2)	108.1(2)	106.1(3)	106.06(14)
C(6)−C(7)−N(1)	111.3(3)	109.8(3)	109.1(5)	109.0(2)
C(2)−C(13)−N(2)	110.1(3)	109.9(3)	109.2(5)	108.6(2)
N(2)−Pt−N(3)	97.17(12)	96.47(10)	97.0 (2)	98.16(7)
N(1)−Pt−N(3)	96.73(12)	99.36(10)	100.6(2)	100.32(7)

these displacements (0.1−0.7 Å) and twist angles (7.6−15.6°) suggests the conformational energies of the complexes are not strongly influenced by variation of these parameters over modest ranges.

In the four crystal structures, the planar pyridyl ligands lie nearly perpendicular to the platinum coordination plane, forming dihedral angles of 89.5° (**2**), 84.5° (**3**), 86.0° (**4**), and 89.0° (**5**). These values are consistent with those observed for related complexes with a bulky tridentate ligand bonded to the platinum center, such as Pt((2,6-CH_2-$PPh_2)_2C_6H_3$)(8-acetamidoquinolinato)$^+$ (87.3°).[15] For complexes with less sterically hindered tridentate ligands, such as 2,6-bis((methylthio)methyl)pyridine (SNS), the dihedral angle shows greater variability, ranging from 55.0 to 89.3°: Pt(SNS)(4-CNpy)$^{2+}$, 63.0, 89.3°; Pt(SNS)(4-COOHpy)$^{2+}$, 55.0°; Pt(SNS)(4-NH_2-py)$^{2+}$, 81.3°; Pt(SNS)(4-Clpy)$^{2+}$, 61.7°; Pt(SNS)(4-CH_3py)$^{2+}$, 79.4°.[18] Similar variation is observed for a series of Pt(phbpy)(L)$^+$ complexes (phbpyH = 6-phenyl-2,2′-bipyridine), where L = pyridine (61.7°), 4-aminopyridine (88°), 2-aminopyridine (65.5°), and 2,6-diaminopyridine (68°).[19] In the latter systems, the orientation of the pyridyl ligand may be influenced by well-known agostic interactions between the NH_2 groups and the platinum center.[15,19,20] In contrast, there is no indication of interaction between the Pt center and the benzylic or hydroxyl H atoms of **5**, supporting the notion that the metal center is not strongly basic.[21] The hydroxyl groups of **5** are directed away from the metal center, forming hydrogen bonds with a triflate O atom and an adjacent complex (O(1)−H(1)···O(4), 2.752(3) Å; O(2)−H(2)···O(4), 2.777(2) Å). Kaim et al. have suggested that a dihedral angle of approximately 70° between the pyridine and phenyl rings in Pt(diimine)$(Ph)_2$ provides optimal overlap between the phenyl rings and the π-system of the diimine ligand.[22] The nearly perpendicular orientation of the pyridyl and phenyl groups in crystals of **2**−**5** is consistent with steric considerations, as well as electronic effects, since the Pt−pyridine π-interactions do not directly compete with the Pt−phenyl π-interactions.[5,20,23]

^{1}H NMR Spectroscopy. The ^{1}H NMR spectra of **2**−**5** in $CDCl_3$ are qualitatively similar to that reported previously for compound **1**.[5] A general labeling scheme for nonequivalent protons (A−F) is shown in Scheme 1. The spectra of **1**−**4** exhibit a doublet and triplet between 6.8 and 7.1 ppm due to the protons on the phenyl ring (A, B). The resonances near 4.3 ppm, arising from the benzylic protons (C), exhibit well-resolved ^{195}Pt satellites with J_{H-Pt} values of 47, 54, 50, and 47 Hz for **1**−**4**, respectively. Two characteristic multiplets between 2.9 and 4.1 ppm are attributable to the diastereotopic protons (D′ and D″) of the α-carbons of the

(18) Marangoni, G.; Pitteri, B.; Bertolasi, V.; Ferretti, V.; Gilli, P. *Polyhedron* **1996**, *15*, 2755−2761.

(19) Yip, J. H. K.; Suwarno; Vittal, J. J. *Inorg. Chem.* **2000**, *39*, 3537−3543.

(20) Albrecht, M.; Dani, P.; Lutz, M.; Spek, A. L.; van Koten, G. *J. Am. Chem. Soc.* **2000**, *122*, 11822−11833.

(21) Jude, H.; Krause Bauer, J. A.; Connick, W. B. *J. Am. Chem. Soc.* **2003**, *125*, 3446−3447.

(22) Klein, A.; McInnes, E. J. L.; Kaim, W. *J. Chem. Soc., Dalton Trans.* **2002**, 2371−2378.

(23) Grove, D. M.; van Koten, G.; Ubbels, H. J. C.; Vrieze, K.; Niemann, L. C.; Stam, C. H. *J. Chem. Soc., Dalton Trans.* **1986**, *4*, 717−724.

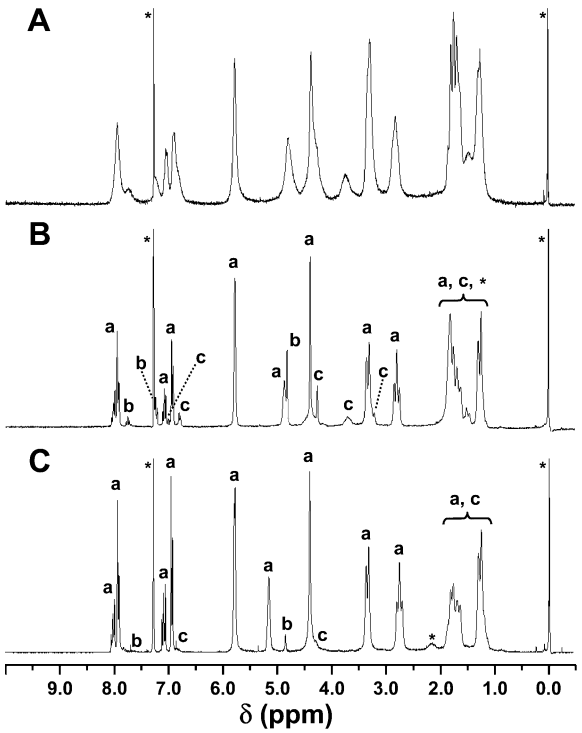

Figure 2. ^{1}H NMR spectra of Pt(pip$_2$NCN)(2,6-pydiol)$^+$ (**5**) in $CDCl_3$ at (A) 298 K, (B) 272 K, and (C) 242 K. Identifiable resonances are labeled for Pt(pip$_2$NCN)(2,6-pydiol)$^+$ (a), 2,6-pydiol (b), and Pt(pip$_2$NCN)(H$_2$O)$^+$ (c), as well as for chloroform, water, and TMS (∗).

piperidyl rings. Similarly, the aliphatic protons E and F are diastereotopic, accounting for the complexity of the splitting patterns further upfield. The aromatic resonances of the pyridyl ligands occur downfield of 7.50 ppm. Notably, the doublet resonance attributable to the α-protons of the pyridyl group (9.0−9.1 ppm) is shifted downfield of the corresponding free ligand resonance, confirming that the pyridyl ligands are bonded to the platinum center. In the case of the 4,4′-bipyridine-bridged dimer (**4**), the pyridyl resonances appear as two doublets at 8.63 and 9.10 ppm, indicating that the two halves of the ligand are equivalent.

In CD_3OD solution, the ^{1}H NMR spectrum of **2** is qualitatively similar to that observed in chloroform. However, the spectra of **3** and **4** indicate that the pyridyl ligands are partially dissociated (<10%) at room temperature. In CD_3CN solution, the dissociation is enhanced, and the NMR spectra of **2**−**4** exhibit resonances associated with the pyridyl complexes, free pyridyl ligand, and Pt(pip$_2$NCN)(H$_2$O)$^+$,[24] as well as the monomeric Pt(pip$_2$NCN)(4,4′-bpy)$^+$ adduct in the case of **4**. These results are consistent with van Koten and van Eldik's assessment of the strong trans-labilizing properties of the NCN$^-$ ligand.[16]

At room temperature, resonances in the ^{1}H NMR spectrum of **5** in $CDCl_3$ solution are broad, as expected for ligand exchange occurring in the slow-to-intermediate exchange regime (Figure 2). All available evidence points to substitution of the pydiol ligand by water that is present as a solvent impurity. At room temperature, compound **5** is the major component in solution. Upon cooling, the resonances sharpen, and those corresponding to compound **5** gain intensity at the expense of the others. At 272 K, resonances attributable to **5**, free pydiol, and Pt(pip$_2$NCN)(H$_2$O)$^+$ are well-resolved. These assignments are confirmed by variable-temperature studies of free pydiol and Pt(pip$_2$NCN)(H$_2$O)$^+$.[24] Taken together with the crystallographic data for **5**, these observations suggest that the bond between the pydiol and the Pt is weakened because of the steric demands of the benzylic groups and the trans-labilizing properties of the NCN$^-$ ligand. In support of this view, the ligand is fully dissociated in CD_3CN solution at room temperature.

Electronic Structures. To investigate their electronic structures, cyclic voltammagrams of **1**−**4** were recorded in methylene chloride solution (0.1 M (TBA)PF$_6$). Compound **1** exhibits an irreversible oxidation near 1.1 V vs Ag/AgCl, similar to that observed for Pt(Me$_4$NCN)Cl (0.76 V vs FcH/FcH$^+$, THF, 0.1 M (TBA)PF$_6$).[25] This behavior is characteristic of metal-centered oxidation of platinum(II) complexes, resulting in large structural reorganization.[26] Similar irreversible waves have been reported for related complexes with NCN$^-$ pincer ligands.[25] At present, no definitive mechanistic information is available for these systems, and a two-electron ECE mechanism is as likely as any other. Nevertheless, the electrochemical behavior of these compounds is markedly different from that observed for nearly reversible cooperative two-electron reagents, such as Pt(2,2′:6′,2″-terpyridine)(pip$_2$NCN)$^+$.[21]

None of the pyridyl complexes (**2**−**4**) undergoes oxidation at potentials <1.3 V, suggesting this process is shifted to more positive potentials, as predicted for neutral donor groups bonded the metal center. As previously noted for **1**,[21] neither **2** nor **3** is reduced at potentials more positive than −1.8 V. However, complex **4** undergoes a nearly reversible one-electron reduction at −1.22 V (ΔE_p = 61 mV, i_{pc}/i_{pa} = 1.4, 0.25 V/s). A similar process has been assigned to a bipyridine-centered reduction in the cyclic voltammagram of [(Pt(PEt$_3$)$_2$)$_4$(μ-4,4′-bpy)$_2$(anthracenyl)$_2$]$^{4+}$ (−1.44 V, ΔE_p = 69 mV, 0.2 V/s, 0.1 M TBAPF$_6$, CH_3CN).[27] Reduction of **4** at potentials more positive than **2** or **3** is in keeping with the relative reduction potentials of the free pyridyl ligands, and the cathodic shift of this process with respect to free 4,4′-bpy is consistent with coordination to the acidic metal centers stabilizing the LUMO of the bridging diimine ligand.

The colorless solids dissolve to give colorless methylene chloride solutions that absorb strongly in the UV region (Figure 3a, Table 3). As noted previously for the chloride

(24) Pt(pip$_2$NCN)(H$_2$O)$^+$ is prepared by reaction of **1** with one equiv of Ag(CF$_3$SO$_3$), in analogy to the synthetic route developed by van Koten and co-workers for the synthesis of Pt(Me$_4$NCN)(H$_2$O)$^+$ (Grove, D. M.; van Koten, G.; Louwen, J. N.; Noltes, J. G.; Spek, A. L.; Ubbels, H. J. C. *J. Am. Chem. Soc.* **1982**, *104*, 6609−6616.)

(25) (a) Back, S.; Gossage, R. A.; Lutz, M.; del Rio, I.; Spek, A. L.; Heinrich, L.; van Koten, G. *Organometallics* **2000**, *19*, 3296−3304. (b) Back, S.; Lutz, M.; Spek, A. L.; Lang, H.; van Koten, G. *J. Organomet. Chem.* **2001**, *620*, 227−234.

(26) (a) Hubbard, A. T.; Anson, F. C. *Anal. Chem.* **1966**, *38*, 1887−1893. (b) Lappin, G. *Redox Mechanisms in Inorganic Chemistry*; Ellis Horwood: New York, 1994.

(27) Kaim, W.; Schwederski, B.; Dogan, A.; Fiedler, J.; Kuehl, C. J.; Stang, P. J. *Inorg. Chem.* **2002**, *41*, 4025−4028.

Table 3. Room-Temperature UV−Visible Absorption (CH_2Cl_2) Spectra, 77 K Emission Data, and Reduction Potentials[c] for **1**−**4**

cmpd (L)	abs λ_{max}, nm (ϵ, cm^{-1} M^{-1})	emission λ_{max}, nm (fwhm, cm^{-1})		$E°$, V
		glassy soln[a]	solid state	
1 (Cl^-)	270 (7800), 281 (8000), 305 sh (2600)	705 (3500)	740	
2 (py)	259 (13 000), 272 sh (8300), 292 sh (3050)	650 (3700)	680	
3 (4-phpy)	262 sh (23 800), 280 (32 100), 286 sh (30 700)	444, 474, 498, 535 sh	450, 477, 508, 546 sh[b]	
4 (4,4-bpy)	260 (30 750), 277 (30 100), 291 sh (24 800), 305 sh (15 800)	433, 458, 485 sh, 520 sh	449, 479, 507, 550sh	−1.44

[a] 4:1 EtOH−MeOH glassy solution. [b] Solid-state maxima of BF_4^- salt. [c] Cyclic voltammograms were recorded in 0.1 M (TBA)PF_6/CH_3CN at 0.25 V/s and referenced vs Ag/AgCl.

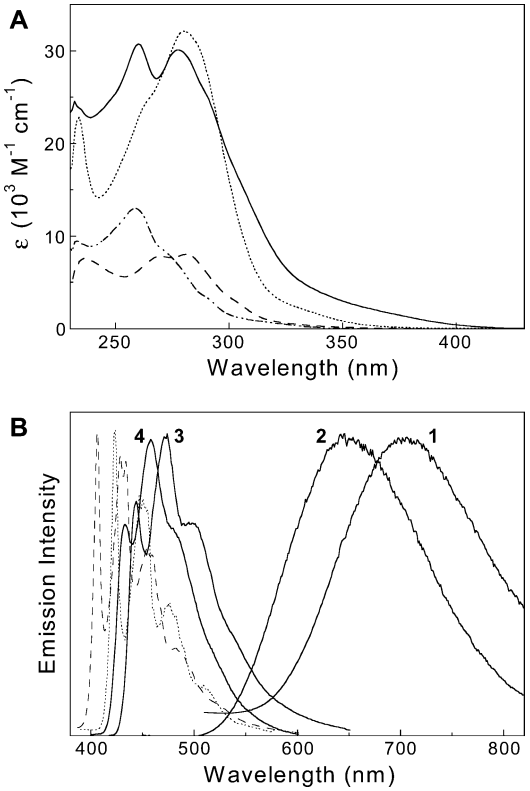

Figure 3. (A) Room-temperature UV−visible absorption spectra in methylene chloride solution for compounds **1** (---), **2** (·· --), **3** (·····), and **4** (—). (B) 77 K emission spectra in 4:1 ethanol−methanol glassy solution for **1**−**4**, 4-phenylpyridine (···) and 4,4′-bipyridine (---). Spectra have been arbitrarily scaled.

complex (**1**) and related compounds,[5,28] the UV spectrum in CH_2Cl_2 is dominated by two intense features (270 nm, 7800 M^{-1} cm^{-1}; 281 nm, 8000 M^{-1} cm^{-1}) tentatively assigned as having partial metal-to-ligand charge-transfer (MLCT) character involving the piperidyl ligand.[5,28,29] As expected for decreased electron density on the metal center, the MLCT bands in the spectrum of the pyridyl complex (**2**) are shifted to shorter wavelengths, and an absorption maximum occurs at 259 nm (13 000 M^{-1} cm^{-1}). The overall absorption profile is remarkably similar to that of the imine analogue, Pt(pip_2-NCN)($CH_3N{=}C(CH_3)_2$)$^+$, in methanol solution (258 nm, 11 000 M^{-1} cm^{-1}; 273 nm, 7600 M^{-1} cm^{-1}; 290 sh nm, 3350 M^{-1} cm^{-1}),[5] as expected for ligands with similar donor properties. The enhanced intensity of the 259 nm absorption for **2** is consistent with an overlapping pyridyl-centered transition that appears in the spectra of free pyridine (252 nm, 2000 M^{-1} cm^{-1}) and protonated pyridine (256 nm, 5360 M^{-1} cm^{-1}, acidic ethanol),[30] as well as other pyridyl complexes.[31−35] Though it is reasonable to expect the MLCT transitions involving the pyridyl ligand to lie between the lowest energy MLCT bands of $Pt(py)_2Cl_2$ (cis, 300 nm; trans, 310 nm)[34] and those of complexes with neutral donor ligands (e.g., $Pt(NH_3)_3(py)^{2+}$, $Pt(NH_3)_2(py)_2^{2+}$, and $Pt(py)_4^{2+}$, <240 nm),[31] the remarkable similarity of the spectra of **2** and the imine analog[5] suggests these bands occur at λ <260 nm for **2**.

The UV spectra of **3** (280 nm, 32 100 M^{-1} cm^{-1}) and **4** (260 nm, M^{-1} cm^{-1}, 30 750 M^{-1} cm^{-1}; 277 nm, 30 100 M^{-1} cm^{-1}) are dominated by bands with significantly greater intensity than observed for **2**, suggesting the presence of additional transitions. Free 4-phpy exhibits a broad $\pi-\pi^*$ absorption near 255 nm (16 600 M^{-1} cm^{-1}) that shifts to 285 nm (∼17 000 M^{-1} cm^{-1}) on protonation.[36] Similar ligand-centered transitions have been identified in the spectra of $Ru(NH_3)_5(4\text{-phpy})^{2+}$ (289 nm, 18 600 M^{-1} cm^{-1}),[37] *fac*-$Re(CO)_3(Cl)(4\text{-phpy})_2$ (268 nm, 36 500 M^{-1} cm^{-1}),[33] and $Cu_4Cl_4(4\text{-phpy})_4$ (286 nm),[38] and a significant fraction of the intensity of the 280 nm feature in the spectrum of **3** is reasonably attributed to a 4-phpy-centered transition. The spectrum of free 4,4′-bpy exhibits an intense $\pi-\pi^*$ absorption band and shoulder (239 nm, 15 400 M^{-1} cm^{-1}; 270 sh nm, ∼6000 M^{-1} cm^{-1}) that also shift slightly to longer wavelengths and gain intensity on double protonation (248 nm, 16 000 M^{-1} cm^{-1}; 275 sh nm, ∼10 000 M^{-1} cm^{-1}).[39] The shorter wavelength band has been identified in the spectra of $Ru(NH_3)_5(4,4'\text{-bpy})^{2+}$ (250 nm, 25700 M^{-1} cm^{-1}),[37] *fac*-$Re(CO)_3(Cl)(4,4'\text{-bpy})_2$ (238 nm, 35 000 M^{-1} cm^{-1}), *fac*-$Re(CO)_3(Cl)(4,4'\text{-bpyH})_2^+$ (∼250 nm),[33] and [$(Ru(NH_3)_5)_2(\mu\text{-}4,4'\text{-bpy})$]$^{4+}$ (249 nm, 15 000 M^{-1} cm^{-1}),[40] and the 260 nm band in the spectrum of **4** is reasonably attributed

(28) van der Ploeg, A. F. M. J.; van Koten, G.; Schmitz, J. E. J.; van der Linden, J. G. M. *Inorg. Chim. Acta* **1982**, *58*, 53−58.
(29) In support of this assignment, comparably intense transitions in the spectrum of Pd(pip_2NCN)Br occur at shorter wavelengths (<270 nm). (Tastan, S.; Connick, W. B. Unpublished results).
(30) Swain, M. L.; Eisner, A.; Woodward, C. F.; Brice, B. A. *J. Am. Chem. Soc.* **1949**, *71*, 1341−1345.
(31) Jørgensen, C. K. *Acta Chem. Scand.* **1957**, *11*, 151−165.
(32) Ford, P. C.; Rudd, D. P.; Gaunder, R.; Taube, H. *J. Am. Chem. Soc.* **1968**, *90*, 1187−1194.
(33) Giordano, P. J.; Wrighton, M. S. *J. Am. Chem. Soc.* **1979**, *101*, 2888−2897.
(34) Martin, M.; Krogh-Jespersen, M.-B.; Hsu, M.; Tewksbury, J.; Laurent, M.; Viswanath, K.; Patterson, H. *Inorg. Chem.* **1983**, *22*, 647−652.
(35) Reimers, J. R.; Hush, N. S. *Inorg. Chem.* **1990**, *29*, 3686−3697.
(36) Favini, G. *Gazz. Chim. Ital.* **1963**, *93*, 635−648.
(37) Lavallee, D. K.; Fleischer, E. B. *J. Am. Chem. Soc.* **1972**, *94*, 2583−2599.
(38) Ryu, C. K.; Kyle, K. R.; Ford, P. C. *Inorg. Chem.* **1991**, *30*, 3982−3986.
(39) Krumholz, P. *J. Am. Chem. Soc.* **1951**, *73*, 3487−3492.
(40) Sutton, J. E.; Sutton, P. M.; Taube, H. *Inorg. Chem.* **1979**, *18*, 1017−1021.

to a 4,4′-bpy-centered transition. Interestingly, an intense longer wavelength $\pi-\pi^*$ feature has not been identified in spectra of the aforementioned complexes; it is conceivable that the broad 280 nm feature in the spectrum of **4** is comprised of several transitions, including a MLCT involving 4,4′-bpy. Though the MLCT bands involving the pyridyl ligands cannot yet be firmly identified for **2**−**4**, the accumulated data suggest that these transitions occur at $\lambda <$ 300 nm (>33 300 cm^{-1}). Assuming singlet−triplet splittings comparable to those reported for other platinum(II) complexes (3000−5000 cm^{-1}),[41,42] the lowest spin-forbidden MLCT absorption band is expected to occur at wavelengths $\lambda <$ 360 nm (>27 800 cm^{-1}) in fluid solution and even shorter wavelengths in rigid matrixes. Thus, given the relatively low energies of the lowest triplet states of the free pyridyl ligands (py, 29 650 cm^{-1}; 4-phpy, 23 800 cm^{-1}; 4,4′-bpy, 24 400 cm^{-1})[43−46] and of the ^{3}LF states of related complexes,[5] it is unlikely that spin-forbidden MLCT emissions will be observed from these complexes.

Solid-state samples of **2** exhibit weak red emissions under UV irradiation at room-temperature, reminiscent of the ^{3}LF emissions observed for **1** and related complexes, Pt(pip$_2$NCN)X (X = Br, I).[5] In contrast, solid-state samples of **3** and **4** exhibit bright yellow-green emission. To investigate the origin of this behavior, the emission spectra of solid and glassy solution samples (4:1 EtOH−MeOH and 2-methyltetrahydrofuran) of **2**−**4** were recorded at 77 K (Figure 3b, Table 3). Solid samples of **2** and **3** showed evidence of contamination consistent with pyridyl ligand substitution.[47] Though dissociation also is expected for solution samples, this chemistry appears to be minimized at low temperatures (Figure 2). In addition, the frozen solution emission profiles are concentration independent and in good agreement with solid-state data, indicating that aggregates are not responsible for the observed spectra.

Excitation of glassy solutions of the triflate salt of **2** at 300 or 355 nm results in characteristically broad, low-energy and Gaussian-shaped emissions centered near 650 nm with a full-width at half-maximum (fwhm) of 3700 cm^{-1}. The emission band exhibits a large Stokes shift from the intense absorption features, and the emission maximum is blue-shifted with respect to that observed for the chloride complex (**1**, 705 nm). Taken together, these observations are consistent with emission originating from a lowest ^{3}LF excited state, as previously reported for **1**.[5] The large Stokes shift and broadness are consistent with an excited state having a optimum geometry very different from that of the ground state, as expected for population of the Pt($d_{x^2-y^2}$) antibonding level. Consequently, the onset of the emission near 515 nm does not necessarily mark the ^{3}LF 0−0 transition, and we can only conclude from these data that the energy of the lowest ligand field state for **2** must be ≥19 400 cm^{-1} (≤515 nm). The 77 K excitation spectra are in good agreement with solution absorption spectra, and at longer wavelengths, a weak band is resolved near 370 nm (**1**, 373 nm; **2**, 365 nm). In the case of **2**, the emission maximum is near that observed for Pt(pip$_2$NCN)(CH$_3$N=C(CH$_3$)$_2$)$^+$ (640 nm), as expected for ligands with comparable donor properties. In the solid state, the emission maxima for **1** (740 nm)[5] and **2** (680 nm) are shifted to longer wavelengths from the frozen solution maxima by ∼700 cm^{-1}. However, in contrast to **1**, the emissions from solid salts of **2** are weakly excitation dependent (e.g., λ_{ex} = 355 nm, λ_{max} = 694 nm), indicating some contamination, presumably from a product of pyridine ligand substitution.[47] In addition, whereas the emission decays for solid samples of **1** are adequately modeled with a single-exponential function (τ, 1.9 μs), the emission decays from repeatedly recrystallized samples of the triflate salt of **2** in glassy solution or the solid state required a biexponential function to obtain a reasonable fit (τ, 3, 11 μs).[47,48] Nevertheless, the microsecond lifetimes are within the expected range for d−d emissions from platinum(II) complexes.[34,49,50]

The intense emissions from glassy solution samples of **3** and **4** excited at 300 nm are strongly blue-shifted with respect to the previous compounds. The sharply structured emissions clearly originate from the lowest pyridyl-centered $\pi-\pi^*$ excited states of the respective 4-phpy and 4,4′-bpy ligands. The ∼1000 and ∼1400 cm^{-1} spacings in the vibronic progressions are in excellent agreement with those of the free ligands (Figure 3b). However, the origin of the bands for **3** and **4** are shifted by ∼1300 and ∼1000 cm^{-1}, respectively, from those of the free ligands, confirming that the observed emissions do not arise from either protonated[51] or free pyridyl ligands (Figure 3b). Similarly, the bandshapes and Franck−Condon factors, as indicated by the Huang−Rhys ratios[52] ($I_{1,0}/I_{0,0}$: **3**, 1.4; **4**, 1.3), are distinctly different from those of the free ligands (0.8, 0.9) and indicative of metal coordination.[41,50,53] The emission spectra of the complexes excited at 355 nm also are several orders of magnitude more intense than those obtained by exciting similar concentrations of 4-phpy and 4,4′-bpy. The excitation spectra are in good agreement with absorption spectra, and in the case of **4**, the emission spectra of solid samples are very similar to those observed for frozen solutions. However, the emissions from salts of **3** show considerable variation depending on counterion and excitation wavelength; it also is likely that sample aging influences these spectra; however, this parameter was not extensively investigated. The emission

(41) Connick, W. B.; Miskowski, V. M.; Houlding, V. H.; Gray, H. B. *Inorg. Chem.* **2000**, *39*, 2585−2592.
(42) Miskowski, V. M.; Houlding, V. H.; Che, C.-M.; Wang, Y. *Inorg. Chem.* **1993**, *32*, 2518−2524.
(43) Evans, D. F. *J. Chem. Soc.* **1959**, 2753−2757.
(44) Hotchandani, S.; Testa, A. C. *J. Photochem. Photobiol., A: Chem.* **1991**, *55*, 353−328.
(45) Bulska, H.; Kotlicka, J. *Pol. J. Chem.* **1979**, *53*, 2103−2115.
(46) Sarkar, A.; Chakravorti, S. *J. Lumin.* **1995**, *65*, 163−168.
(47) The accumulated data are consistent with partial displacement of pyridine by water/anion to give a complex with a lowest d−d emissive state; multistate emission as reported for[34] *cis*-Pt(py)$_2$Cl$_2$ is an alternative explanation.
(48) Demas, J. N. *Excited-State Lifetime Measurements*; Academic Press: New York, 1983.
(49) Diomedi Camassei, F.; Ancarani-Rossiello, L.; Castelli, F. *J. Lumin.* **1973**, *8*, 71−81.
(50) Miskowski, V. M.; Houlding, V. H. *Inorg. Chem.* **1989**, *28*, 1529−1533.
(51) Yagi, M.; Matsunaga, M.; Higuchi, J. *Chem. Phys. Lett.* **1982**, *86*, 219−222.
(52) Huang, K.; Rhys, A. *Proc. R. Soc. London* **1950**, *204A*, 406−423.
(53) Ohno, T.; Kato, S. *Bull. Chem. Soc. Jpn.* **1974**, *47*, 2953−2957.

decay for **4** in the solid state is adequately modeled by a single-exponential function (τ, 0.16 ms), whereas the decay for **3** is not (τ, 0.1, 0.6 ms). Nevertheless, as expected for a lowest triplet excited state centered on the pyridyl ligands, the observed lifetimes are significantly shorter than those of the free ligands (4-phpy, 2.1 s; 4,4′-bpy, 0.8 s)[46] but considerably longer than observed for **1** and **2**.

The accumulated data indicate that substitution of pyridine with 4-phenylpyridine in $Pt(pip_2NCN)L^+$ complexes results in a dramatic change in the orbital character of the emissive state. To a reasonable approximation, the donor properties of the two pyridyl ligands are simlar, and the crossover from a lowest, ^{3}LF state to a $^3\pi-\pi^*$ state can be largely attributed to the $\sim$5900 cm^{-1} stabilization[43,44,46] of the triplet $\pi-\pi^*$ state of 4-phpy with respect to that of py. (Similarly, the lowest triplet state of 4,4′-bpy lies $\sim$5300 cm^{-1} below that of py.)[45,46] Though the large Stokes shift of ^{3}LF emissions makes difficult the evaluation of the 0−0 energy of the emitting state of **2**, the preceding results effectively bracket this energy between the emission onset for compounds **3** and **4** ($\sim$425 nm, 23 500 cm^{-1}) and the lowest triplet state of py (337 nm, 29 650 cm^{-1}).

Acknowledgment. Diffraction data were collected through the Ohio Crystallographic Consortium, funded by the Ohio Board of Regents 1995 Investment Fund (CAP-075) and located at the University of Toledo, Instrumentation Center in A&S, Toledo, OH 43606. W.B.C. thanks the National Science Foundation (Grant CHE-0134975) for their generous support and the Arnold and Mabel Beckman Foundation for a Young Investigator Award. H.J. and W.B.C. are grateful to the University of Cincinnati University Research Council for summer research fellowships. H.J. thanks the University of Cincinnati Department of Chemistry for the Stecker Fellowship, the Link Foundation for an Energy Fellowship, and the University of Cincinnati for a Distinguished Dissertation Fellowship. We thank Drs. H. B. Mark, M. J. Baldwin, R. C. Elder, E. Brooks, and M. J. Goldcamp, as well as Ms. S. Mandel and Mr. Sudhir Shori, for helpful discussions and expert technical assistance.

Supporting Information Available: Tables of crystallographic data, structure refinement details, atomic coordinates, interatomic distances and angles, anisotropic displacement parameters, and calculated hydrogen parameters in CIF format. This material is available free of charge via the Internet at http://pubs.acs.org.

IC0346329